ELSEVIER

Earth and Planetary Science Letters 208 (2003) 297–304

EPSL

www.elsevier.com/locate/epsl

Simulation of solute transport in discrete fracture networks using the time domain random walk method

Jacques Bodin *, Gilles Porel, Fred Delay

UMR 6532 Hydrasa, Université de Poitiers, Bât. Sciences Naturelles, 40 av. Recteur Pineau, 86022 Poitiers Cedex, France

Received 22 August 2002; received in revised form 22 January 2003; accepted 27 January 2003

Abstract

The time domain random walk (TDRW) method has been developed for simulating solute transport in discrete fracture networks. The following transport processes have been considered: advective transport in fractures, hydrodynamic dispersion along the fracture axis, sorption reactions on the fracture walls and decay reactions. The TDRW method takes advantage of both random walk and particle-tracking methods. It allows for the one-step calculation of the particle residence time in each bond of the network while avoiding mass balance problems at fracture intersections with contrasted dispersion coefficients. The accuracy of the TDRW method has been addressed by means of synthetic test problems into single fractures and into a 2D discrete fracture network. In each case, simulated and theoretical results compare very well.

Keywords: fracture network; solute transport; Lagrangian simulation

1. Introduction

Simulation of solute transport in fractured rocks is a basic requirement for two present-day issues: groundwater pollution in fractured aquifers and performance assessment of radioactive waste repositories in crystalline rocks. As transport in such media is often advection-dominated, Lagrangian methods are attractive because they are free of numerical dispersion. The simplest Lagrangian models rest on particle-tracking routines, which assume plug flow where dispersion at the local scale is negligible compared to dispersion resulting from the heterogeneity of the flow field [1–3]. However, this assumption is questionable, particularly when dealing with pollutant transport. For instance, the arrival times from a pollution source to a well for water supply may be underestimated and lead to tragic consequences. Moreover, in the case of radioactive leakage from a repository for spent nuclear fuel, the radioactivity level of the solute that arrives in the biosphere may be much more important than that predicted by pure advection in fractures. Note that particle-tracking routines can be adapted to include the effects of both velocity profiles between the fracture walls and of molecular diffusion. In that case,

* Corresponding author. Tel.: +33-54-9454106; Fax: +33-54-9454241.
E-mail addresses: jacques.bodin@hydrasa.univ-poitiers.fr (J. Bodin), gilles.porel@hydrasa.univ-poitiers.fr (G. Porel), frd@ccr.jussieu.fr (F. Delay).

0012-821X/03/$ – see front matter
doi:10.1016/S0012-821X(03)00052-9

the particles are moved by advection along path lines and random jumps are superimposed to simulate diffusion over path lines. This approach is justified for simulating the dispersion at the scale of the fracture plane. However, it is time-consuming and not suited to complex fracture networks.

To take into account dispersion in single fractures, transport models may be built using the classic random walk (RW) method instead of the particle-tracking method. The RW method is based on the stochastic motion of a large number of particles, which obeys a Markovian process. In one dimension, this process can be written as:

$$X_p(t+\Delta t)-X_p(t)=\mu_x+Z\sigma_x \quad (1)$$

and satisfies the 1-D Fokker–Planck equation:

$$\frac{\partial \psi}{\partial t}=-\frac{\partial(v\psi)}{\partial x}+\frac{1}{2}\frac{\partial^2(\phi\psi)}{\partial x^2} \quad (2)$$

where $v=\mu_x/\Delta t$; $\phi=\sigma_x{}^2/\Delta t$; $X_p(\tau)$ [L] is the position of the particle at time τ, μ_x [L] is the mean displacement of particles during time step Δt [T], $\sigma_x{}^2$ [L^2] is the variance of the particle motion during Δt, Z is a random number drawn from a normal deviate and ψ is the probability density function of the particle displacements. The parameters v and ϕ are chosen so that Eq. 2 corresponds to the advection–dispersion equation, which is straightforward when the advection–dispersion equation in the fracture plane is written in the form:

$$\frac{\partial c_f}{\partial t}=-\frac{\partial}{\partial x}\left[\left(u_f+\frac{\partial D_f}{\partial x}\right)c_f\right]+\frac{\partial^2(D_f c_f)}{\partial x^2} \quad (3)$$

where c_f [M L^{-3}] is the solute concentration in the fracture, t the time variable, x [L] the space coordinate along the flow direction, u_f [L T^{-1}] the mean fluid velocity and D_f [L^2 T^{-1}] the hydrodynamic dispersion coefficient. Thus, the calculation of particle displacements is performed as follows [4]:

$$X_p(t+\Delta t)-X_p(t)=\left[u_f+\frac{\partial D_f}{\partial x}\right]\Delta t+Z\sqrt{2D_f\Delta t} \quad (4)$$

The main difficulty in RW simulations lies in the particle transition between two media with contrasted dispersion coefficients. If the transition is abrupt, the derivative of the dispersion coefficient in Eq. 4 is not defined, the mass balance at the interface is not preserved, and special techniques have to be applied to compute the particle leaps. Since dispersion in fractures is generally velocity-dependent ($D_f \propto u_f^n$, with $0 \le n \le 2$, see Detwiler et al. [5]), this problem is particularly emphasized in fracture networks because fluid velocity may differ by several orders of magnitude from one fracture to the next, which leads to sharp contrasts in dispersion coefficients. Both interpolation and reflection techniques have been proposed to overcome this problem [6–8]. However, these methods increase the computing time because time steps have to be refined for preserving the mass balance at the interface. Moreover, the RW method necessitates at least 30 leaps per particle in a bond to simulate dispersion accurately. With realistic fracture networks of thousands of bonds, this yields cumbersome calculations.

In this work, we have developed a Lagrangian method in time domain taking advantage from both random walk and particle-tracking methods. The time domain random walk (TDRW) method was first introduced by Banton et al. [9] for simulating non-reactive solute transport in 1-D porous media. Delay and Bodin [10] proposed a first extension of this method, enabling the simulation of transport in a single fracture, while accounting for matrix diffusion. Here, the TDRW method has been adapted to discrete fracture networks and enhanced to deal with sorption and decay reactions. The particle travel time between two nodes of the network is calculated in one step while taking into account the mechanisms mentioned above. This avoids the multiple-leap calculations of classical RW methods and strongly reduces computation efforts.

2. The TDRW method

The fracture network is represented by connected bonds with 1-D flow and the following mechanisms are considered: advection in fractures, hydrodynamic dispersion along the fracture plane, adsorption on the fracture walls and radio-

active decay. The fluid velocity is assumed to be constant in each bond of the fracture network (i.e. between two successive fracture intersections). The adsorption reaction obeys a linear instantaneous equilibrium. To consider a one-dimensional transport along the fractures, it is stated that: (1) the width of each fracture is much smaller than its length, and (2) transverse diffusion and dispersion within each fracture ensure complete mixing across its width. The transport in bonds is then described by:

$$\frac{\partial c_f}{\partial t} + \lambda c_f = -\frac{u_f}{R_f}\frac{\partial c_f}{\partial x} + \frac{1}{R_f}\frac{\partial}{\partial x}\left(D_f \frac{\partial c_f}{\partial x}\right) \quad (5)$$

where λ [T^{-1}] is the decay constant and R_f [dimensionless] is the retardation coefficient which represents the effect of solute sorption on the fracture walls. In the Lagrangian framework, considering the change of variable:

$$\frac{\partial c_f}{\partial t} = \frac{\partial c_f}{\partial x}\frac{\partial x}{\partial t} = \frac{\partial c_f}{\partial x}\frac{u_f}{R_f} \quad (6)$$

Eq. 5 can be rewritten as:

$$\frac{\partial c_f}{\partial x} + \lambda c_f \frac{R_f}{u_f} = -\frac{R_f}{u_f^2}\frac{\partial}{\partial t}\left[\left(u_f + \frac{\partial D_f}{\partial x}\right)c_f\right] + \frac{R_f^2}{u_f^3}\frac{\partial^2}{\partial t^2}(D_f c_f) \quad (7)$$

Terms in Eq. 7 can be identified with those in the Fokker–Planck equation by applying an equivalent change of variable to Eq. 2:

$$\frac{\partial \psi}{\partial x} = -\frac{1}{v^2}\frac{\partial (v\psi)}{\partial t} + \frac{1}{2v^3}\frac{\partial^2(\phi\psi)}{\partial t^2} \quad (8)$$

Thus, the mean and variance of the particle travel time distribution for a displacement of length Δx are respectively:

$$\mu_t = \frac{R_f}{u_f^2}\left(u_f + \frac{\partial D_f}{\partial x}\right)\Delta x \quad (9)$$

$$\sigma_t^2 = R_f^2 \frac{2D_f \Delta x}{u_f^3} \quad (10)$$

However, while the Markovian process in Eq. 1 leads to a Gaussian distribution of particles in space, it can be shown that the travel time distribution is lognormal for Peclet numbers $Pe = u_f \Delta x / D_f$ larger than 10 (see Appendix). Therefore, the stochastic calculation of travel times over a distance Δx is given by:

$$\ln(\Delta t_{\Delta x}) = \mu_{ln} + Z\sigma_{ln} \quad (11a)$$

$$\mu_{ln} = \ln\left(\mu_t / \sqrt{1 + \sigma_t^2/\mu_t^2}\right) \quad (11b)$$

$$\sigma_{ln}^2 = \ln(1 + \sigma_t^2/\mu_t^2) \quad (11c)$$

where μ_t and σ_t^2 are the mean and variance in Eqs. 9 and 10, $\Delta t_{\Delta x}$ [T] the particle travel time for a travel distance Δx, Z a random number drawn from a normal deviate, and μ_{ln} [T] and σ_{ln}^2 [T^2] the mean and variance of the logtransform. If indices n and $n+1$ refer to the upstream and downstream nodes of a bond of length Δx, the particle travel time in this bond is:

$$t_{n+1} - t_n = \exp(\mu_{ln} + Z\sigma_{ln}) \quad (12)$$

Note that the TDRW method enables the scale-dependent dispersion coefficient to be dealt with, provided that the spatial derivative in Eq. 9 is calculable. The decay reaction is simulated by computing the mass decrease of the particle:

$$mp_{n+1} = mp_n \exp[-\lambda (t_{n+1} - t_n)] \quad (13)$$

where mp_n and mp_{n+1} [M] represent the mass of the particle at nodes n and $n+1$, respectively.

The assumption made on the form of the travel time distribution is the main limitation of the TDRW method. Indeed, in fracture networks, Peclet numbers can be locally less than 10 in very short bonds or in bonds with very low flow velocities. The assumption of a lognormal travel time distribution in these bonds can be erroneous, and yield inaccurate results. However, we have found that an empirical correction of Eq. 11b makes it possible to preserve the accuracy of the TDRW method for $Pe < 10$. This corrections consists in multiplying Eq. 11b by a factor $\beta = 1 - 1/(33Pe)$, which leads to:

$$\mu_{ln}^* = \beta \mu_{ln} = \left(1 - \frac{1}{33Pe}\right)\ln\left(\frac{\mu_t}{\sqrt{1 + \sigma_t^2/\mu_t^2}}\right) \quad (14)$$

The use of Eq. 14 instead of Eq. 11b will be illustrated in Section 3. Other limitations may stem from the assumption of a full mixing across the width of each fracture, required for considering 1-D transport. The validity of this assumption is questionable in short bonds with high flow velocities, because the transit time along these bonds can be lower than the mixing time across the aperture. However, this problem is strongly damped in realistic fracture networks, because the time spent by a particle in these bonds is very low as compared to its total residence time in the network.

3. First validation of the TDRW method: transport in a single fracture

The ability of a model to simulate transport in a fracture network depends first on its accuracy in each elementary bond. To check this point, three theoretical transport problems in a single fracture were simulated. For the first two tests, the solute was assumed to undergo first-order radioactive decay and sorption reactions on the fracture walls. The case of an instantaneous injection at the inlet of the fracture was first addressed. Assuming a steady-state flow in the fracture and a constant dispersion coefficient, the breakthrough curve at the fracture outlet can be computed with the analytical solution of the advection–dispersion equation for 1-D semi-infinite media [11]:

$$c_{f1}(t) = \frac{m_0 l_f}{2bWu_f\sqrt{4\pi\frac{D_f}{R_f}t^3}} \exp\left(-\frac{\left(l_f-\frac{u_f}{R_f}t\right)^2}{4\frac{D_f}{R_f}t}\right)\exp(-\lambda t) \quad (15)$$

where m_0 [M] is the injected mass, l_f [L] the fracture length, b [L] the half-aperture of the fracture and W [L] the fracture width. The second transport problem was based on the same assumptions as above, except that the injection followed an exponential decaying release $F(t) = m_0\gamma\exp(-\gamma t)$ where F [M T^{-1}] is the solute mass flux at the inlet of the fracture, m_0 [M] the total mass injected in the fracture and γ [T^{-1}] a decay coefficient defining the release rate of the injected mass and also accounting for the radioactive decay of the source mass. In that case, the theoretical breakthrough curve can be computed by applying the convolution theorem to Eq. 15:

$$c_{f2}(t) = \int_0^t \frac{F(\tau)}{m_0} c_{f1}(t-\tau)\,d\tau \quad (16)$$

With the TDRW method, a non-instantaneous injection can be simulated by assigning a delayed initial time to each particle. For the exponential decaying injection described above, a random initial time T_{init} was thus computed for each particle according to the following expression:

$$T_{init} = -\frac{1}{\gamma}\log(Z_{01}) \quad (17)$$

where Z_{01} is a random number drawn from a uniform deviate between 0 and 1. The parameter values used in both problems were arbitrarily fixed as follows: $m_0 = 10^{-3}$ g; $l_f = 10$ m; $2b = 2.5\times10^{-4}$ m; $W = 1$ m; $u_f = 4\times10^{-5}$ m s^{-1}; $D_f = 2\times10^{-5}$ m^2 s^{-1}; $R_f = 1.2$; $\lambda = 3\times10^{-6}$ s^{-1}; $\gamma = 1\times10^{-5}$ s^{-1}. The third problem was set up to test the accuracy of the TDRW method for very low Peclet numbers, using Eq. 14 instead of Eq. 11b. A transport problem in a small bond has been carried out with Pe = 2, that is: $l_f = 1$ m; $u_f = 4\times10^{-5}$ m s^{-1}; $D_f = 2\times10^{-5}$ m^2 s^{-1}, and an instantaneous injection of non-reactive tracer (no radioactive decay and no sorption reactions). The results of the three tests are shown in Figs. 1 and 2. The very good match between numerical and analytical results proves the accuracy of the TDRW method, whatever the Peclet number values.

4. Second validation of the TDRW method: transport in a discrete fracture network

To check the efficiency of the TDRW method in simulating transport in fractured rocks, a series of numerical tests was performed on a 2-D synthetic fracture network with two orthogonal sets of fractures (Fig. 3). Fracture apertures were constant and equal to 2.5×10^{-4} m. The fractured

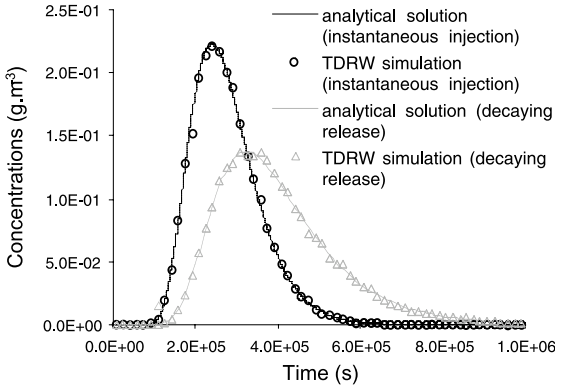

Fig. 1. Solute transport in a single fracture with sorption on the fracture walls and radioactive decay. Comparison between TDRW simulations (30 000 particles) and analytical breakthrough curves.

block was subjected to a steady-state flow and the boundary conditions were: constant hydraulic heads of 100 m and 95 m on sides 1 (north) and 3 (south), respectively, and no flow conditions on sides 2 and 4 (east and west). The hydraulic heads at the nodes of the network were calculated using Darcy's law, a mass conservation principle at fracture intersections (i.e. Kirchoff's law) and a direct method to solve the system of linear equations. Then, fluid velocities in the bonds were calculated using a parallel plate approximation and the Hagen–Poiseuille flow $u_n = (H_{n+1} - H_n)\rho g b^2/(3\mu l_n)$ where H_n and H_{n+1} [L] are the hydraulic heads at nodes n and $n+1$, ρ [M L^{-3}] the fluid density, b [L] the half-aperture of the fracture, μ [M L^{-1} T^{-1}] the dynamic viscosity and l_n [L] the

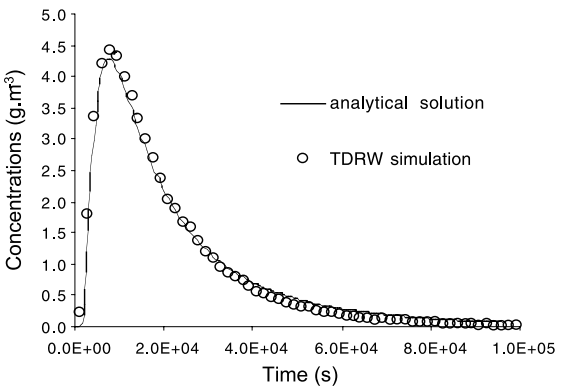

Fig. 2. Example of the accuracy of the TDRW method for a low Peclet number (Pe = 2).

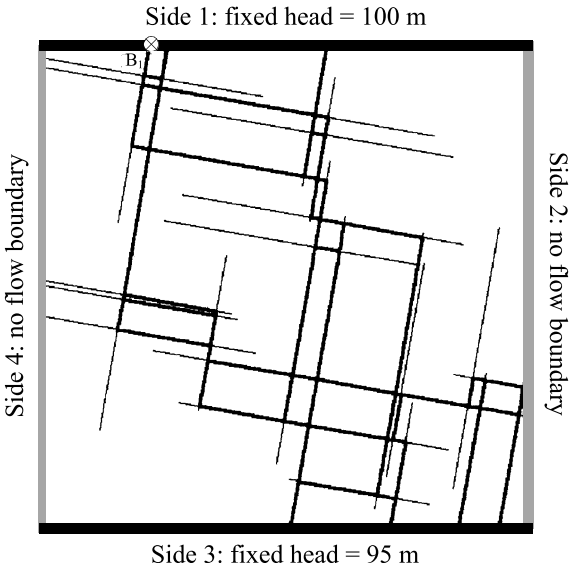

Fig. 3. The network test problem for TDRW simulations: size = 350 × 350 m; 27 fractures. The 71 bold lines show the flowing bonds, i.e. the backbone of the network. The tracer particles were injected at the inlet of bond B_1.

length of the bond (n, $n+1$). A total mass $m_0 = 10^{-2}$ g represented by 50 000 particles was injected into one of the flowing fractures intersecting side 1, and the TDRW breakthrough curves were computed at the outlet of the network (side 3, see Fig. 3). A sharp contrast of dispersivity (ratio of 20) between both orthogonal sets of bonds was assumed. A constant dispersivity of 2 m was assigned to bonds N–S, whereas the dispersivity in bonds E–W was fixed at 0.1 m. Two TDRW simulations were performed in the network, considering either the perfect mixing or the stream-tube assumption for mass sharing at fracture intersections [12]. The CPU time required for TDRW simulations was approximately 9 s with an 850-MHz Pentium® III PC, which reduces the calculation time by a factor 30 as compared to a standard random walk method.

Note that a more general mixing model was recently proposed by Park and Lee [13] but perfect mixing and stream-tube assumptions, which are extreme cases, are more relevant to test the TDRW method. The complex issue of the actual tracer behavior at these intersections is beyond the purpose of the present work. Park et al. [14] have shown this topic to be of weak influence in

most fracture networks, as compared to variability and uncertainty in parameters defining the geometrical structure of networks.

To get the analytical solutions at the scale of the fracture network, the latter was split into elementary paths. An elementary path is defined as a set of flowing bonds connected in series through which a particle may cross the network (Fig. 4). In well-connected systems, the number of such paths is generally much greater than the number of flowing bonds. For instance, 1800 elementary paths were identified as compared to 71 flowing bonds in the simple network of Fig. 3. For a non-reactive tracer, the solute mass flux at the second node of an elementary path, denoted F_2 [M T^{-1}] is given by:

$$F_2(t) = \frac{m_0 l_1}{\sqrt{4\pi D_1 t^3}} \exp\left(-\frac{(l_1 - u_1 t)^2}{4 D_1 t}\right) \tag{18}$$

where l_1 [L] is the length of the first bond in the elementary path, u_1 [L T^{-1}] the fluid velocity in the first bond and D_1 [L^2 T^{-1}] the dispersion coefficient in the first bond. The solute transport into the elementary path can be modeled by applying the convolution theorem:

$$F_{n+1}(t) = \int_0^t \varepsilon_n F_n(\tau) E_n(t-\tau)\,\mathrm{d}\tau = \varepsilon_n F_n(t) * E_n(t) \tag{19}$$

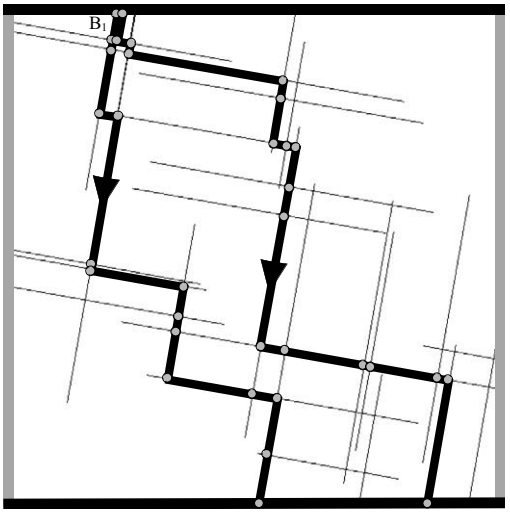

Fig. 4. Two distinct elementary paths.

where '$*$' symbolizes the convolution operator; F_n and F_{n+1} [M T^{-1}] are the solute mass flux at nodes n and n+1; ε_n is the percentage of the solute mass in bond (n−1, n) that flows into bond (n, n+1), this percentage depends on the flow configuration and on the mixing model at the fracture intersection; E_n [T^{-1}] is the probability density function of residence times in bond (n, n+1). For a non-reactive solute, $E_n(t)$ is:

$$E_n(t) = \frac{l_n}{\sqrt{4\pi D_n t^3}} \exp\left(-\frac{(l_n - u_n t)^2}{4 D_n t}\right) \tag{20}$$

where l_n [L] is the length of bond (n, n+1), u_n [L T^{-1}] the fluid velocity in bond (n, n+1) and D_n [L^2 T^{-1}] the dispersion coefficient in bond (n, n+1). For an elementary path i with N bonds in series, the solute mass flux across the outlet may be calculated from the residence time distributions in each individual bond. Given that Eq. 18 may be rewritten as: $F_2(t) = m_0 E_1(t)$, the recursive application of Eq. 19 through the N nodes gives:

$$F_N(t) = m_0 \left(\prod_{j=2}^{N-1} \varepsilon_j\right) E_1(t) * E_2(t) \ldots * E_{N-1}(t) \tag{21}$$

Because the time spent by a particle in bond (n−1, n) has no influence on its time spent in bond (n, n+1), time distributions are statistically independent. In that case, the means and variances of residence times in successive bonds are additive [15]. Therefore, the convolution product in Eq. 21 can be replaced by an equivalent probability density function:

$$E_{\mathrm{eq}}(t) = \frac{l_{\mathrm{eq}}}{\sqrt{4\pi D_{\mathrm{eq}} t^3}} \exp\left(-\frac{(l_{\mathrm{eq}} - u_{\mathrm{eq}} t)^2}{4 D_{\mathrm{eq}} t}\right) \tag{22a}$$

where:

$$l_{\mathrm{eq}} = \sum_{j=1}^{N} l_j \tag{22b}$$

$$u_{\mathrm{eq}} = \frac{l_{\mathrm{eq}}}{\bar{t}_{\mathrm{eq}}} = \frac{l_{\mathrm{eq}}}{\sum_{j=1}^{N} \bar{t}_j} = \frac{l_{\mathrm{eq}}}{\sum_{j=1}^{N} (l_j/u_j)} \tag{22c}$$

$$\sigma^2_{\mathrm{eq}} = \sum_{j=1}^{N} \sigma_j^2 = \sum_{j=1}^{N} \frac{2 D_j l_j}{u_j^3} \tag{22d}$$

$$D_{eq} = \frac{u_{eq}^3 \sigma_{eq}^2}{2 l_{eq}} \quad (22e)$$

The theoretical breakthrough curve at the downstream boundary of the network is the sum of the elementary solutions of each path. Using in the notations an additional exponent i referring to the paths, the concentration at the outlet is:

$$c_{out}(t) = \frac{\sum_{i=1}^{NbP} F_{Ni}^{i}(t)}{\sum_{i=1}^{NbP} Q^{i}} = \frac{m_0}{Q_{Tot}} \sum_{i=1}^{NbP} \left[\left(\prod_{j=2}^{N_i - 1} \varepsilon_j^i \right) E_{eq}^{i}(t) \right] \quad (23)$$

where Q^i [L^3 T^{-1}] is the flow rate into the elementary path i, Q_{Tot} [L^3 T^{-1}] the total flow rate into the network, N_i the total number of bonds in the elementary path i and NbP the total number of elementary paths. Results of TDRW simulations and analytical breakthrough curves calculated with Eq. 23 are plotted in Fig. 5. Once again, numerical results compare very well with analytical results, for both the perfect mixing and stream-tube models at fracture intersections. This confirms the accuracy of the TDRW method and proves its efficiency for simulating advective–dispersive transport in fracture networks.

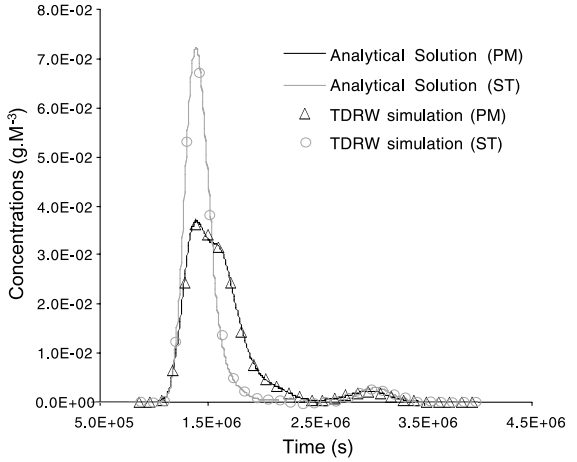

Fig. 5. Comparison between TDRW simulations (50 000 particles) and analytical breakthrough curves at the outlet of the network. PM: perfect mixing assumption; ST: stream-tube assumption.

5. Conclusion

An efficient Lagrangian method developed in time domain is proposed for the simulation of solute transport in discrete fracture networks. The method handles both advection and dispersion mechanisms and allows the particle residence times to be directly computed in each bond of the network. Comparisons between numerical results and analytical breakthrough curves for single fractures and discrete networks have proven the accuracy of the method. Transport simulations are free of numerical dispersion, are much faster than the classic RW method and avoid mass balance problems stemming from dispersion contrast at fracture intersections. Thus, the method is expected to be very useful for simulating solute transport in complex 2-D fracture networks or 3-D channel networks. Other mechanisms such as radioactive decay, sorption reactions or scale-dependent dispersion are easily accounted for. Because these mechanisms often influence tracer test experiments, at either the laboratory or field scale, the TDRW method should become a convenient tool to fit and interpret real-case studies.

Acknowledgements

We are grateful to the French National Program for Research in Hydrology for the financial support of this work.***[BARD]***

Appendix. Lognormal distribution of travel times

The TDRW method assumes that the travel time distribution in 1-D flowing bonds is lognormal. An empirical justification is that classical breakthrough curves show a positive asymmetry. This is reinforced by the comparison of skewness and kurtosis coefficients between a theoretical travel time distribution and a lognormal one.

The probability density function of travel times in a semi-infinite 1-D medium is:

$$f(x,t) = \frac{x}{\sqrt{4\pi\frac{D}{R}t^3}} \exp\left(-\frac{\left(x-\frac{u}{R}t\right)^2}{4\frac{D}{R}t}\right) \quad (24)$$

with x the travel distance, u the mean fluid velocity [L T^{-1}], D the dispersion coefficient [L^2 T^{-1}], and R [dimensionless] the retardation coefficient which represents the effect of solute sorption along the flow path. Using the temporal centered moments: $\mu_n = \int_0^\infty f(x,t)(t-\bar{t})^n \, dt$ with $\bar{t} = \int_0^\infty f(x,t)t \, dt = Rx/u$, the skewness coefficient γ_1 and the kurtosis coefficient γ_2 of Eq. 24 are calculated as:

$$\gamma_1 = \frac{\mu_3}{(\mu_2)^{3/2}} = \sqrt{\frac{18}{\mathrm{Pe}}} \quad (25)$$

$$\gamma_2 = \frac{\mu_4}{(\mu_2)^2} - 3 = \frac{30}{\mathrm{Pe}} \quad (26)$$

with the Peclet number $\mathrm{Pe} = ux/D$. On the other hand, a lognormal distribution of mean $t_m = Rx/u$ and of variance $\sigma_t^2 = 2R^2Dx/u^3$ has a skewness coefficient γ'_1 and a kurtosis coefficient γ'_2 given by:

$$\gamma'_1 = \frac{\sigma_t(3t_m^2 + \sigma_t^2)}{t_m^3} = \sqrt{\frac{18}{\mathrm{Pe}}} + \sqrt{\frac{8}{\mathrm{Pe}^3}} \quad (27)$$

$$\gamma'_2 = \frac{\sigma_t^2(16t_m^6 + 15t_m^4\sigma_t^2 + 6t_m^2\sigma_t^4 + \sigma_t^6)}{t_m^8}$$

$$= \frac{32}{\mathrm{Pe}} + \frac{60}{\mathrm{Pe}^2} + \frac{48}{\mathrm{Pe}^3} + \frac{16}{\mathrm{Pe}^4} \quad (28)$$

It is obvious that Eqs. 25 and 27 and Eq. 26 and 28 result in almost the same values whenever $\mathrm{Pe} > 10$, which is the case for most transport problems in fractures.

References

[1] M.C. Cacas, E. Ledoux, G. de Marsily, A. Barbreau, P. Calmels, B. Gaillard, R. Margritta, Modeling fracture flow with a stochastic discrete fracture network: Calibration and validation, 2, The transport model, Water Resour. Res. 26 (1990) 491–500.

[2] L. Moreno, I. Neretnieks, Fluid flow and solute transport in a network of channels, J. Contam. Hydrol. 14 (1993) 163–192.

[3] Y.W. Tsang, C.F. Tsang, A particle-tracking method for advective transport in fractures with diffusion into finite matrix blocks, Water Resour. Res. 37 (2001) 831–835.

[4] W. Kinzelbach, The random walk method in pollutant transport simulation, in: E. Custodio, A. Gurgui, J.P. Lobo Ferreira (Eds.), Groundwater Flow and Quality Modeling, D. Reidel, Norwell, MA, 1988, pp. 227–245.

[5] R.L. Detwiler, H. Rajaram, R.J. Glass, Solute transport in variable-aperture fractures: An investigation of the relative importance of Taylor dispersion and macrodispersion, Water Resour. Res. 36 (2000) 1611–1625.

[6] E.M. LaBolle, J. Quastel, G.E. Fogg, Diffusion theory for transport in porous media: Transition-probability densities of diffusion processes corresponding to advection-dispersion equations, Water Resour. Res. 34 (1998) 1685–1693.

[7] P. Ackerer, R. Mose, Comment on 'Diffusion theory for transport in porous media: Transition-probability densities of diffusion processes corresponding to advection-dispersion equations' by Eric M. Labolle et al, Water Resour. Res. 36 (2000) 819–821.

[8] E.M. LaBolle, G.E. Fogg, Reply on Comment by P. Ackerer and R. Mose on 'Diffusion theory for transport in porous media Transition-probability densities of diffusion processes corresponding to advection-dispersion equations' by E. LaBolle et al, Water Resour. Res. 36 (2000) 823–824.

[9] O. Banton, F. Delay, G. Porel, A new time domain random walk method for solute transport in 1-D heterogeneous media, Ground Water 35 (1997) 1008–1013.

[10] F. Delay, J. Bodin, Time domain random walk method to simulate transport by advection-dispersion and matrix diffusion in fracture networks, Geophys. Res. Lett. 28 (2001) 4051–4055.

[11] J. Bear, Dynamics of Fluids in Porous Media, Elsevier, New York, 1972, 764 pp.

[12] B. Berkowitz, C. Naumann, L. Smith, Mass transfer at fracture intersections: An evaluation of mixing models, Water Resour. Res. 30 (1994) 1765–1773.

[13] Y.J. Park, K.K. Lee, Analytical solutions for solute transfer characteristics at continuous fracture junctions, Water Resour. Res. 35 (1999) 1531–1537.

[14] Y.J. Park, J.R. de Dreuzy, K.K. Lee, B. Berkowitz, Transport and intersection mixing in random fracture networks with power law length distributions, Water Resour. Res. 37 (2001) 2493–2501.

[15] A. Rasmuson, Analysis of hydrodynamic dispersion in discrete fracture networks using the method of moments, Water Resour. Res. 21 (1985) 1677–1683.